Interaction of electromagnetic waves and suprathermal electrons in the near-critical electric field limit

Interaction of electromagnetic waves and suprathermal electrons in the near-critical electric field limit

Journal of Physics: Conference Series **401** (2012) 012012 doi:10.1088/1742-6596/401/1/012012

Interaction of electromagnetic waves and suprathermal electrons in the near-critical electric field limit

A Kómár[1], G I Pokol[1] and T Fülöp[2]

[1] Department of Nuclear Techniques, Budapest University of Technology and Economics, Association EURATOM, H-1111 Budapest, Hungary

[2] Department of Applied Physics, Nuclear Engineering, Chalmers University of Technology and Euratom-VR Association, Göteborg, Sweden

E-mail: komar@reak.bme.hu

Abstract. The velocity-space anisotropy of suprathermal electron distributions is a source of free energy that may destabilize plasma waves through a resonant interaction between the waves and the energetic electrons. In this work we use a suprathermal electron distribution appropriate for the case when the accelerating electric field is near-critical and we investigate the frequencies, wave numbers and propagation angles of the most unstable waves using a general dispersion relation. It is shown that if the electric field is sub-critical, the anisotropy is not enough to drive electromagnetic waves unstable, as the Landau damping of the waves overwhelms the drive through the anomalous Doppler resonance. In the case when the electric field is super-critical, two types of electromagnetic waves will be destabilized, the electron-whistler and the extraordinary electron wave. The number of electrons for destabilization of the latter is several orders of magnitude lower than for the electron-whistler wave. Consequently, the threshold for destabilization of the extraordinary electron wave is much lower.

1. Introduction

Magnetically confined plasmas often have suprathermal electron populations accelerated by electric fields induced in magnetic reconnection. If the electric field is larger than a certain critical field (E_c), the accelerating force overwhelms the friction for high energy electrons, and these electrons can run away. In tokamak disruptions, the electric field is often well above the critical field and these fields can accelerate electrons to relativistic energies and may generate a runaway electron current exceeding 1 MA. During normal operation the electric field is not as high as in a disruption, but it may nevertheless transiently exceed the critical field and accelerate electrons. There are several experimental observations that suprathermal electrons are produced during the sudden plasma cooling at magnetic reconnection events in sawtooth crashes [1, 2]. Estimates show that in these cases the electric field induced by the sawtooth crash is much larger than the critical one, and generates a suprathermal electron distribution. The steady-state on-axis electric field is close to the critical in these cases and this prevents a deceleration of the electrons between the sawtooth crashes.

The distribution of the suprathermal electrons has an anisotropy in velocity space and through this, they may drive electromagnetic waves unstable via a resonant interaction, not only when the electric field is far above the critical [3, 4, 5] but also in the near-critical case [6, 7]. In this work we generalize and extend the formalism describing the wave-particle interaction in the near-critical case by using a general dispersion relation and investigating also a case when the electric field is close to critical but is not quite as large as that (subcritical case).

2. Suprathermal distribution function in the subcritical case

In recent work [8], analytical expressions have been derived for the electron distribution function in plasmas where the electric field is close to critical, $\alpha \sim 1$, where $\alpha = E/E_c = 4\pi\epsilon_0^2 m_e c^2 E/n_e e^3 \ln\Lambda$. Here, n_e is the thermal electron density, m_e is the electron rest mass, e is the electron charge, $\ln\Lambda$ is the Coulomb logarithm, ϵ_0 is the dielectric constant and c is the speed of light. The distribution function of the suprathermal electrons in the slightly subcritical case ($\alpha \lesssim 1$) is obtained by matching solutions of the Fokker-Planck equation in different regions of momentum space and can be written as

$$f_{\rm st} = \exp F = \exp\left(\epsilon^{-1}F^{(0)} + \epsilon^{-1/2}F^{(1)} + F^{(2)} + ... + C_{\rm st}\right), \tag{1}$$

where $\epsilon = E_c/E_D \ll 1$, E_D is the Dreicer field, $F^{(0)}$, $F^{(1)}$, $F^{(2)}$ are given by Eqs. (23), (37)-(38) and the normalization constant $C_{\rm st}$ is defined by Eqs. (39) and (9) of Ref. [8]. Figure 1a shows a contour-plot of this distribution for $\alpha = 0.9$. The distribution is only slightly anisotropic, which is to be expected because of the subcritical value of the electric field.

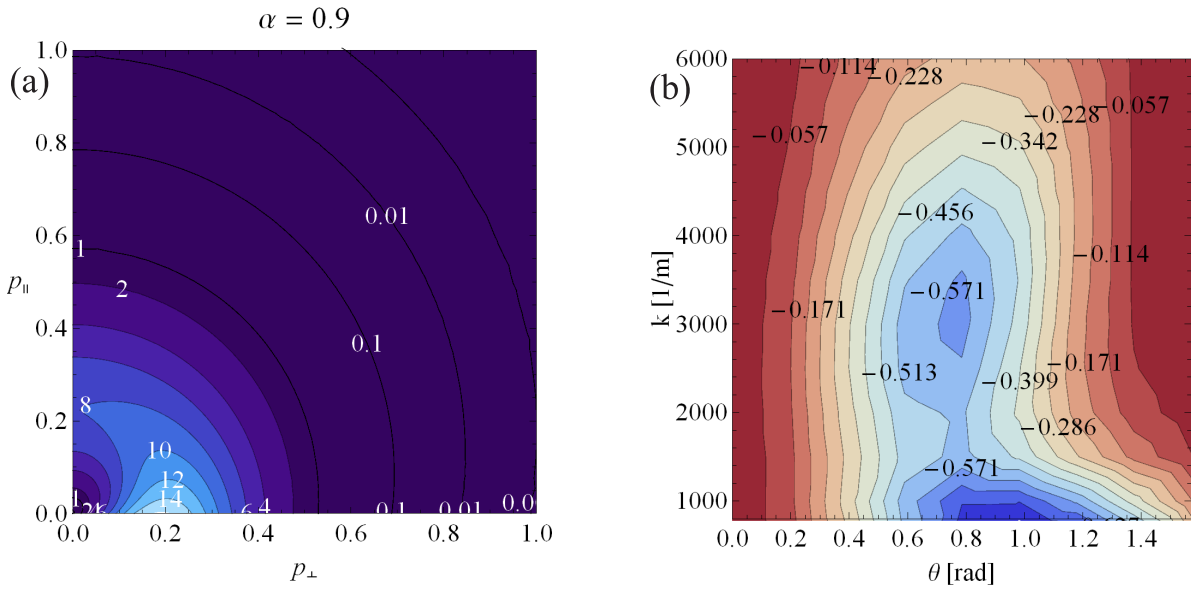

Figure 1. (a) Suprathermal electron distribution for $\alpha = 0.9$, plotted with respect to the parallel and perpendicular momentum normalized to $m_e c$. (b) Growth rate ($10^3\gamma_i/\omega_{ce}$) of the electron-whistler wave for suprathermal electrons, sum of the anomalous-Doppler and Cherenkov resonances. The parameters are $\alpha = 0.9$, $Z = 1$ effective ion charge, $n_e = 5 \cdot 10^{19}$ m^{-3} thermal electron density and $B = 2$ T magnetic field.

It should be noted that the $f_{\rm st}$ suprathermal distribution function is only valid for normalized relativistic momenta $p = \gamma v/c \sim \mathcal{O}(1)$.

Using this electron distribution we can calculate the linear growth rates for the high-frequency electromagnetic waves through a perturbative analysis similar to the one presented in [7]. Using the electromagnetic approximation, $\epsilon_{33}^{e+i} \gg k_\parallel k_\perp c^2/\omega^2$, leads to the dispersion relation $(\epsilon_{11} - k_\parallel^2 c^2/\omega^2)(\epsilon_{22} - k^2 c^2/\omega^2) + \epsilon_{12}^2 = 0$, where ω is the wave frequency, k is the wave number, where the $\parallel$ index denotes its component parallel to the static magnetic field and $\boldsymbol{\epsilon}$ is the dielectric tensor of the plasma, consisting of the susceptibilities of the different plasma species: $\boldsymbol{\epsilon} = \mathbf{1} + \boldsymbol{\chi}^i + \boldsymbol{\chi}^e + \boldsymbol{\chi}^r$, the indices i, e and r denoting the ion, thermal electron and runaway population. Throughout this work we used the cold plasma approximation for the ion and

thermal electron susceptibilities [9] which was seen to be accurate for temperatures up to 20 keV [7]. The dispersion relation can be further simplified using the approximation $\omega \gg \omega_{ce}\sqrt{m_e/m_i}$, for which the unperturbed dielectric tensor is $\epsilon_{11}^{e+i} = 1-\omega_{pe}^2/(\omega^2-\omega_{ce}^2)$, $\epsilon_{22}^{e+i} = 1-\omega_{pe}^2/(\omega^2-\omega_{ce}^2)$, $\epsilon_{12}^{e+i} = -i\omega_{pe}^2\omega_{ce}/[\omega(\omega^2-\omega_{ce}^2)]$, where ω_{pe} is the electron plasma- and ω_{ce} is the electron cyclotron frequency. This dispersion defines three different electromagnetic waves, of which it was shown that if $\alpha \gtrsim 1$ the lowest frequency branch, the so-called 'electron-whistler wave', was most unstable. The perturbative effect of the runaway electrons is taken into account by including the runaway susceptibility [7] in the dielectric tensor. This results in the changing of the wave frequency by a $\delta\omega$ term, the imaginary part of which is the linear growth rate of the wave.

Figure 1b shows that the linear growth rates excited by suprathermal electrons with the distribution (1) (valid for $\alpha \lesssim 1$) are negative on the whole wave number and propagation angle plane, where $\theta = k_\parallel/k$. This was somewhat unexpected, as it was shown in [6, 7] that for runaway electrons in a slightly higher electric field (near-critical case with $\alpha \gtrsim 1$) the corresponding growth rates are positive. The only part of the calculation different from the $\alpha \gtrsim 1$ case was the distribution function, which appears only in the anisotropy term of the runaway susceptibilities: $\mathcal{A} \equiv n\omega_{ce}\partial f/\partial p_\perp + kc\cos\theta\, p_\perp \partial f/\partial p_\parallel$. In the case of $\alpha \gtrsim 1$, this term was positive for both $n = 0$ (Cherenkov resonance) and $n = -1$ (anomalous-Doppler resonance), while in the $\alpha \lesssim 1$ case, the term is negative for $n = 0$ and positive for $n = -1$. The anomalous-Doppler term is negligible compared to the negative growth rate due to the Cherenkov resonance and therefore the waves in the subcritical case are stable.

3. Runaway distribution function

As we have established that the suprathermal populations that are formed in a sub-critical case are stable, we now turn our attention to the runaway distribution, the expression for which is also given in Ref. [8] as

$$f_r(p_\parallel, p_\perp) = \frac{A}{p_\parallel^{(C_s-2)/(\alpha-1)}} \exp\left(-\frac{(\alpha+1)p_\perp^2}{2(1+Z)p_\parallel}\right) {}_1F_1\left(1-\frac{C_s}{\alpha+1}, 1; \frac{(\alpha+1)p_\perp^2}{2(1+Z)p_\parallel}\right), \qquad (2)$$

where $C_s = \alpha - \frac{(1+Z)}{4}(\alpha-2)\sqrt{\frac{\alpha}{\alpha-1}}$, Z is the effective ion charge, ${}_1F_1$ is the confluent hypergeometric function [10] and A is a normalization constant. Because of the continuous acceleration of electrons due to the constant electric field more and more electrons will run away, thus the integral of the distribution is divergent. However, in reality the electric field is constant only for a finite time, then drops. Therefore, the number of runaway electrons and their maximum energy will have an upper limit they can possibly reach. The value of this limit, $p_{\max}$ depends on the exact value and time evolution of the accelerating field. In this paper we will use $p_{\max} = 5$ corresponding to the maximum energy 2.6 MeV.

The distribution is positive on all of the momentum space only if the first argument of ${}_1F_1$ is positive: $C_s < \alpha + 1$. Furthermore, the condition $f_r \to 0$ for $p_\parallel \to \infty$ requires that $C_s > 2$. This distribution was used in [6, 7] to study the destabilization of the electron-whistler and magnetosonic-whistler waves. However, if the electromagnetic approximation breaks down, other waves may be driven unstable. In the following we will use the full dispersion relation to study the interaction of runaway electrons with the electromagnetic waves.

4. Wave dispersion

The full dispersion relation is the following:

$$\left[\left(\epsilon_{11} - \frac{k_\parallel^2 c^2}{\omega^2}\right)\left(\epsilon_{22} - \frac{k^2c^2}{\omega^2}\right) + \epsilon_{12}^2\right]\left(\epsilon_{33} - \frac{k_\perp^2 c^2}{\omega^2}\right) - \frac{k_\parallel^2 k_\perp^2 c^4}{\omega^4}\left(\epsilon_{22} - \frac{k^2c^2}{\omega^2}\right) = 0. \qquad (3)$$

In order to proceed with the calculation of the growth rate we rewrite this dispersion relation, by substituting the formulas for the dielectric tensor elements, and arrive at: $\omega^8 - \omega^6\left(2k^2c^2+\omega_{ce}^2+3\omega_{pe}^2\right) + \omega^4\left[k^4c^4+2k^2c^2(\omega_{ce}^2+2\omega_{pe}^2)+\omega_{pe}^2(\omega_{ce}^2+3\omega_{pe}^2)\right] - \omega^2\left[k^4c^4(\omega_{ce}^2+\omega_{pe}^2)+k^2c^2\omega_{pe}^2(3/2\omega_{ce}^2+2\omega_{pe}^2+1/2\omega_{ce}^2\cos 2\theta)+\omega_{pe}^6\right] = -1/2k^4c^4\omega_{ce}^2\omega_{pe}^2(1+\cos 2\theta)$. This dispersion gives four different branches of electromagnetic waves, three of which have already been studied in Refs. [6, 7] and one new branch. These are plotted on Fig. 2, where the lowest frequency branch is the previously named 'electron-whistler wave', and the second lowest is the new branch, which we will call 'extraordinary electron wave', as this is described in Ref. [9] as a high-frequency extraordinary wave.

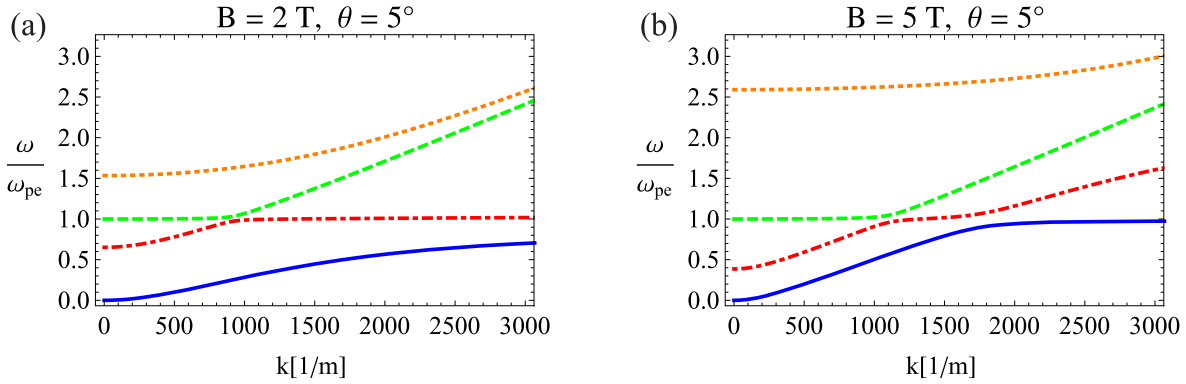

Figure 2. Wave dispersion of the electromagnetic waves at $\theta = 5$ degrees propagation angle for (a) $B = 2$ T and (b) $B = 5$ T. The thermal electron density is $n_e = 5 \cdot 10^{19}$ m^{-3}. The solid blue line corresponds to the electron-whistler wave and the red dashed line is the extraordinary electron wave. The branches with higher frequencies are not destabilized by the suprathermal electrons.

In the presence of runaway electrons, the linear growth rate of the waves can be calculated by perturbing the dispersion with the runaway susceptibility [7]. This results in an additional $\delta\omega$ term in the wave frequency, the imaginary part of which is the linear growth rate γ_i. The growth rate is then given by

$$\frac{\gamma_i}{\omega^6\left(\omega^2-\omega_{ce}^2\right)} = \Im\left\{-\chi_{11}\left(\epsilon_{11}-k^2c^2/\omega^2\right)\left(\epsilon_{33}-k_\perp^2c^2/\omega^2\right) - 2\chi_{12}\epsilon_{12}\left(\epsilon_{33}-k_\perp^2c^2/\omega^2\right) - \chi_{22}\left[\left(\epsilon_{11}-k_\parallel^2c^2/\omega^2\right)\left(\epsilon_{33}-k_\perp^2c^2/\omega^2\right) - k_\parallel^2k_\perp^2c^4/\omega^4\right] - \chi_{33}\left[\epsilon_{11}^2-\epsilon_{11}\left(k^2c^2/\omega^2+k_\parallel^2c^2/\omega^2\right)+k^2k_\parallel^2c^4/\omega^4+\epsilon_{12}^2\right]\right\}/P(\omega,k,\theta), \quad (4)$$

where $P(\omega,k,\theta) = 8\omega^7 - 6\omega^5\left(2k^2c^2+\omega_{ce}^2+3\omega_{pe}^2\right) + 4\omega^3\left[k^4c^4+2k^2c^2(\omega_{ce}^2+2\omega_{pe}^2)+\omega_{pe}^2(\omega_{ce}^2+3\omega_{pe}^2)\right] - 2\omega\left[k^4c^4(\omega_{ce}^2+\omega_{pe}^2)+k^2c^2\omega_{pe}^2(3/2\omega_{ce}^2+2\omega_{pe}^2+1/2\omega_{ce}^2\cos 2\theta)+\omega_{pe}^6\right]$.

The growth rates of the two highest frequency branches were already discussed in Ref. [7] and it has been concluded that these cannot be destabilized by the runaway population. Thus we turn our attention to the remaining two branches, the electron-whistler and the extraordinary electron wave.

The growth rate of the electron-whistler wave is plotted on Fig. 3 for two different magnetic fields. These growth rates do not differ much from the growth rate calculated with the simplified dispersion [6, 7], neither qualitatively nor quantitatively for $B = 2$ T, but as we will show later the parameters and growth rate of the most unstable wave differ for magnetic fields larger than

$B \gtrsim 2.5$ T. The parameters of the most unstable wave are determined by the maximum energy of the runaway electrons [7]. In Fig. 3 this quantity is chosen to be 2.6 MeV, corresponding to $p_{\max} = 5$, and the corresponding $k - \theta$ curve is plotted with a white dotted line on Fig. 3a, while it corresponds to such high wave numbers for $B = 5$ T that it cannot be seen on Fig. 3b. By decreasing the maximum energy, the wave number of the most unstable wave increases while its propagation angle decreases, resulting in the increasing frequency of the most unstable electron-whistler wave [7].

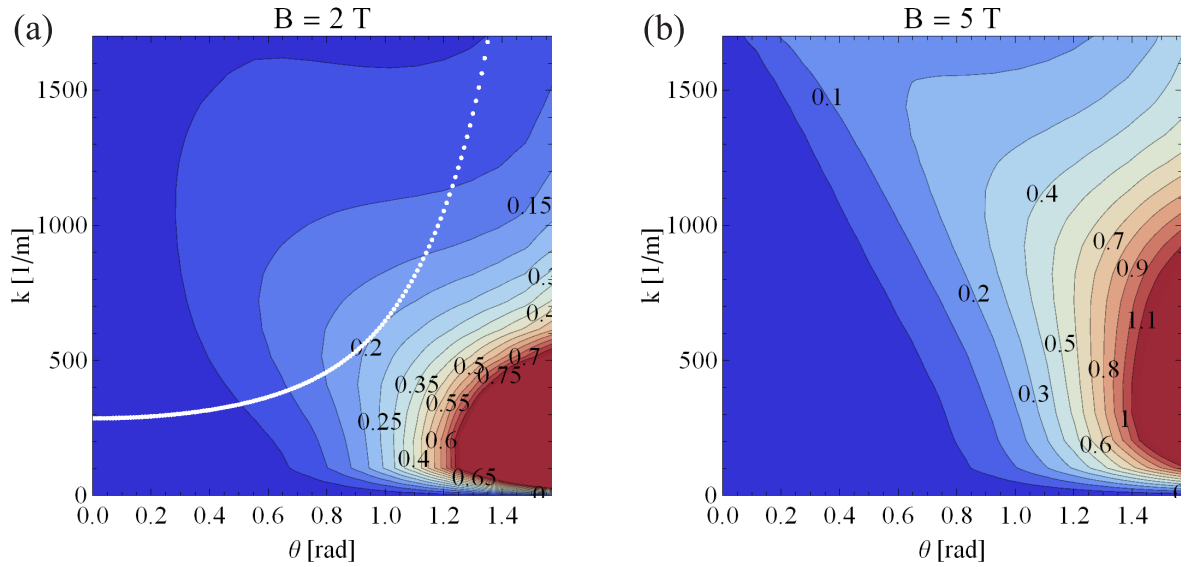

Figure 3. Growth rates ($10^2\gamma_i/\omega_{ce}$) for the electron-whistler wave with the full dispersion (contour lines) and the $k - \theta$ values corresponding to $p_{\max} = 5$ (white dotted line). Growth rate (a) for $B = 2$ T, (b) for $B = 5$ T magnetic field, sum of the anomalous-Doppler and Cherenkov resonances. The parameters are $\alpha = 1.3$, $Z = 1$, $n_e = 5 \cdot 10^{19}$ m^{-3}, $n_r = 3 \cdot 10^{17}$ m^{-3} runaway density and $p_{\max} = 5$.

By comparing the growth rate of the electron-whistler wave in the near-critical case to the growth rate of the magnetosonic-whistler wave in the high electric field case previously investigated [3, 4, 5] we can conclude that the growth rates are qualitatively similar in the two cases, having a maximum at low wave numbers and near-perpendicular propagation. For a high enough $p_{\max}$ this maximum of the growth rate would define the most unstable wave even in the near-critical case. Based on this and the qualitatively similar runaway distributions in the two cases, a smooth transition can be envisioned in between, for arbitrary electric fields. The quasilinear evolution of the whistler wave has already been investigated for high electric fields in Ref. [4] and it was found that the destabilization of the whistler wave led to the scattering of the runaway electrons in velocity space. Due to the similarities in the two cases, we expect that the effect of this interaction would be similar in the near-critical case, in the sense that a scattering of the runaway electrons would occur, while this effect would possibly be slower and less dominant.

The extraordinary electron wave can be destabilized only in a limited region of the $k - \theta$ parameter space and has a positive growth rate in this region, see Fig. 4. As in the case of the electron-whistler, the most unstable wave is determined by the maximum runaway energy, however, there is a difference in the two cases. While the electron-whistler wave can be destabilized on the whole $k - \theta$ parameter space, thus by runaways with arbitrary maximum energy, the extraordinary electron wave cannot be destabilized by runaways with energies higher

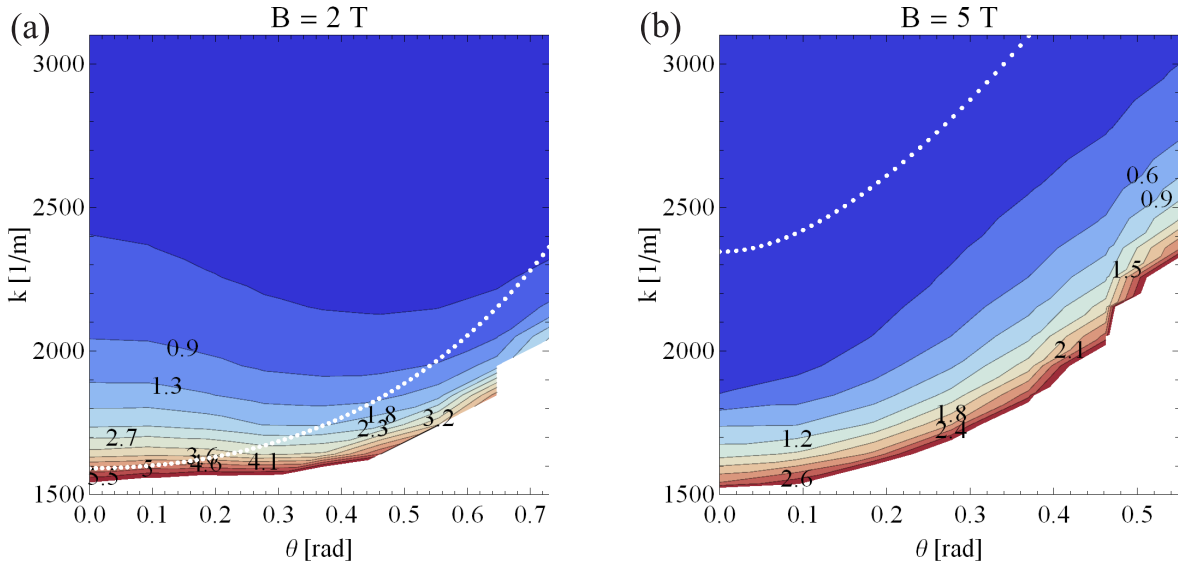

Figure 4. Growth rates ($10^2\gamma_i/\omega_{ce}$) for the extraordinary-electron wave with the full dispersion (contour lines) and the $k-\theta$ values corresponding to $p_{\max} = 5$ (white dotted lines). Growth rate (a) for $B = 2$ T, (b) for $B = 5$ T magnetic field, sum of the anomalous Doppler and Cherenkov resonances. The parameters are $\alpha = 1.3$, $Z = 1$, $n_e = 5 \cdot 10^{19}$ m^{-3}, $n_r = 3 \cdot 10^{17}$ m^{-3} and $p_{\max} = 5$.

than 2.6 MeV for the parameters in the figure caption (for $B = 2$ T). This is due to the restriction posed on the growth rate by the resonance condition: in order to have a real and positive resonant momentum certain limitations apply for the wave dispersion [7].

If we compare the growth rates of the electron-whistler and the extraordinary electron wave, we can conclude that for $p_{\max} = 5$ the most unstable extraordinary electron wave has a growth rate an order of magnitude higher than the electron-whistler wave.

5. Stability

By comparing the instability growth rate of the electron-whistler wave and the extraordinary electron wave to the various damping rates, we can determine a stability threshold for the destabilization of these waves. By taking into account collisional (γ_d) and convective damping (γ_v), a wave is unstable if $\gamma_l = \gamma_i - \gamma_d - \gamma_v > 0$. Collisional damping equals to $\gamma_d = 1.5\tau_{ei}^{-1}$ [11], where $\tau_{ei} = 3\pi^{3/2} m_{e0}^2 v_{Te}^3 \epsilon_0^2 / n_i Z^2 e^4 \ln\Lambda$ is the electron-ion collision time. This is the dominant damping mechanism in cold plasmas. The convective damping term takes into account the effect that wave energy is transported out of the runaway beam with the group velocity $\partial\omega/\partial k_\perp$, and equals to $\gamma_v \equiv (\partial\omega/\partial k_\perp)/(4L_r)$, where L_r is the radius of the runaway beam [5].

The growth rates of the most unstable waves driven by a near-critical electron distribution with $p_{\max} = 5$ were compared to the collisional and convective damping rates for $T_e = 20$ eV post-disruption electron temperature and for $T_e = 1$ keV temperature, and the obtained stability thresholds are shown in Fig. 5. If the runaway density is higher than the critical values plotted in Fig. 5, the corresponding wave is destabilized.

Fig. 5a shows the critical runaway densities for the destabilization of the electron-whistler wave. By comparing this to the stability thresholds calculated in Refs. [6, 7] with the simplified dispersion, it can be seen that the two cases differ both quantitatively and qualitatively for high magnetic fields. In Fig. 5a, the stability threshold decreases for increasing magnetic field for values higher than 3.5 T.

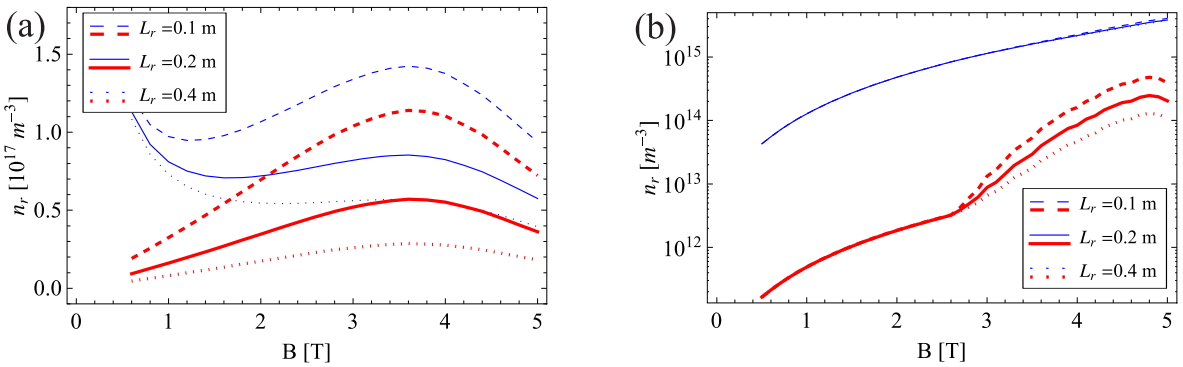

Figure 5. Stability thresholds in near-critical electric field. (a) Thresholds for the most unstable electron-whistler wave, (b) for the most unstable extraordinary electron wave as a function of the magnetic field. The electron temperatures are $T_e = 20$ eV (blue thin lines) and $T_e = 1$ keV (red thick lines). The runaway-beam radius is $L_r = 0.1$ m (dashed), $L_r = 0.2$ m (solid) and $L_r = 0.4$ m (dotted). The other parameters are $\alpha = 1.3$, $Z = 1$, $n_e = 10^{20}$ m^{-3} and maximum runaway energy of 2.6 MeV, corresponding to $p_{\max} = 5$.

On Fig. 6 the parameters and growth rate of the most unstable electron-whistler wave are shown for the (3) full dispersion and the simplified dispersion given in Section 2, as well as the convective damping of these waves. It can be seen that for higher magnetic fields these start to differ, and the most dominant effect behind the decrease in the stability threshold in Fig. 5a is that the growth rate of the wave (given by (3), the full dispersion relation) increases. This is due to two facts: (1) the parameters of the most unstable wave are different for high magnetic fields, while they are the same for low magnetic fields (see Fig. 6ab), and (2) the growth rate of the full dispersion increases faster with the magnetic field than the growth rate of the simplified dispersion.

On Fig. 5b stability thresholds are shown for the extraordinary electron wave. The critical density needed to destabilize this wave increases with the magnetic field. For 1 keV background temperature, the increase in the critical density suffers a break around 2.5 T, which is due to the corresponding break in the convective damping of the most unstable wave (see the dash-dotted line in Fig. 6d). This jump in the critical density becomes more dominant with increasing temperature, while it disappears at low temperatures, see the lines corresponding to 20 eV in Fig. 5b. By comparing the order of magnitude of the critical densities for the extraordinary electron wave to that of the electron-whistler, we can conclude that the extraordinary electron wave is more likely to be destabilized, as it has several order of magnitudes lower critical density.

6. Conclusions

Our results show that if the electric field is sub-critical, suprathermal electrons do not destabilize electromagnetic waves. In contrast, if the electric field is super-critical, both the electron-whistler wave and the extraordinary electron wave are destabilized. The extraordinary electron wave is a new branch, which is only present if the electromagnetic approximation is relaxed and the general wave dispersion is used. The wave number and propagation angle of the most unstable extraordinary electron wave is very different from its electron-whistler counterpart. It propagates almost parallel to the magnetic field if $B \lesssim 2.5T$. Above $B \simeq 2.5T$, the propagating angle becomes larger and this leads to a considerable increase in the convective damping. The extraordinary electron wave is much easier to destabilize than the electron-whistler branch. Interestingly, the stability threshold of the extraordinary electron wave exhibits a clear threshold at $B_{tr} \simeq 2.5$ T if the electron temperature is higher than 500 eV. Considerably fewer electrons

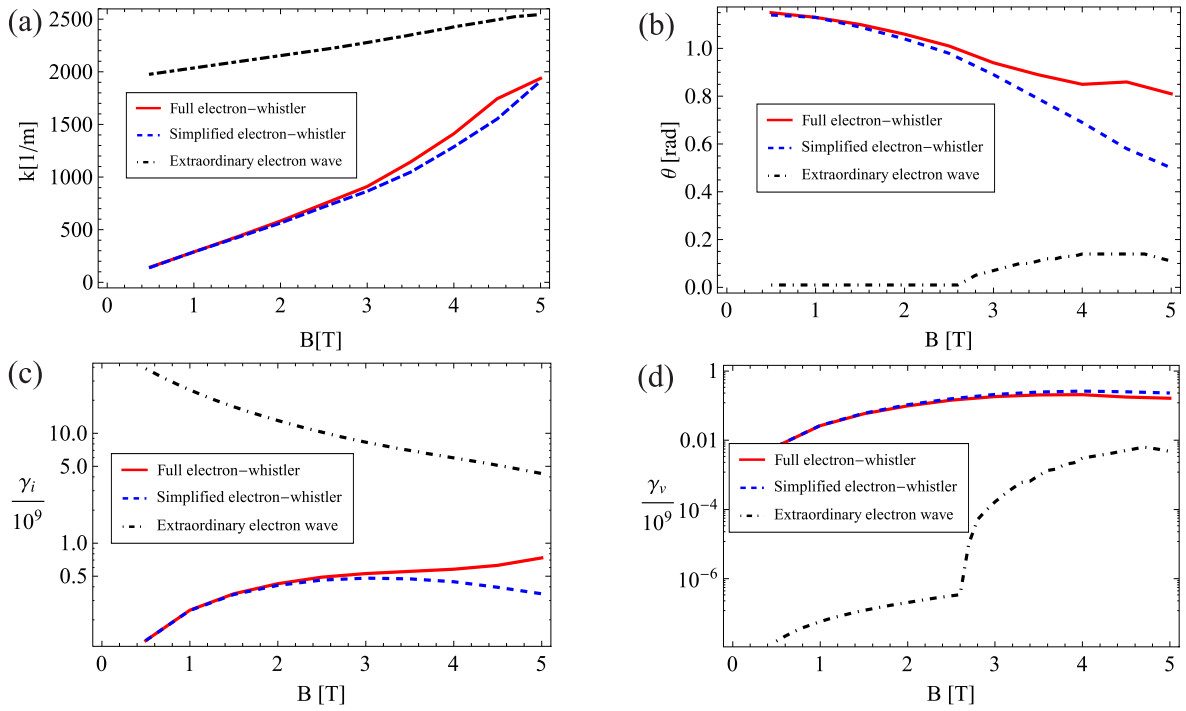

Figure 6. Parameters, growth rate and convective damping of the most unstable electron-whistler and extraordinary electron wave. (a,b) Parameters of the most unstable wave. (c,d) Growth rate and convective damping for the most unstable wave. The parameters are $\alpha = 1.3$, $Z = 1$, $n_e = 10^{20}$ m^{-3}, $n_r = 3 \cdot 10^{17}$ m^{-3}, $p_{\max} = 5$ and $L_r = 0.1$ m.

are needed for destabilization of this wave below B_{tr} than above. Destabilization of this wave is expected to lead to pitch-angle scattering of the runaway electron beam and therefore may be part of the reason for the observed magnetic field threshold for runaway beam formation in large tokamaks [12, 13].

Acknowledgments

This work was funded by the European Communities under Association Contract between EURATOM, HAS and *Vetenskapsrådet*. One of the authors acknowledges the financial support of the grant TÁMOP-4.2.2/B-10/1-2010-0009.

References

[1] Savrukhin P V, *Phys. Rev. Letters*, **86** (2001) 3036.
[2] Klimanov I, Fasoli A, Goodman T P, *Plasma Phys. Control. Fusion*, **49** (2007) L1.
[3] Fülöp T et al., *Phys. Plasmas* **13**, 062506 (2006).
[4] Pokol G et al., *Plasma Phys. Control. Fusion* **50**, 045003 (2008).
[5] Fülöp T et al., *Phys. Plasmas* **16**, 022502 (2009).
[6] Kómár A et al, in Proc. of the 39th European Physical Society meeting on Plasma Physics and 16th International Congress on Plasma Physics. P5.043 (2012);
[7] Kómár A et al, submitted to *Phys. Plasmas* (2012).
[8] Sandquist P et al., *Phys. Plasmas*, **13** 072108 (2006).
[9] Stix T H, Waves in plasmas, *American Institute of Physics*, New York (1992).
[10] Abramowitz M and Stegun I A, editors, *Handbook of Mathematical Functions*, chapter 13, page 503 (1972).
[11] Brambilla M, *Phys. Plasmas* **2**, 1094 (1995).
[12] Gill R D et al., *Nucl. Fusion* **42**, 1039 (2002).
[13] Yoshino R et al., *Nucl. Fusion* **39**, 151 (1999).